

Fabrication of Aluminum/Gr Composites and Investigation of its Tribological and Wear Properties

M. Heydari Vini*

Department of Mechanical Engineering,

Islamic Azad University, Mobarakeh branch, Isfahan, Iran

E-mail: m.heydari@mau.ac.ir

*Corresponding author

Received: 13 August 2022, Revised: 26 January 2023, Accepted: 10 February 2023

Abstract: Nowadays metal matrix composites are popular in many industries due to their desirable properties. Severe plastic deformation techniques usually are popular to fabricate metal matrix composites. In this study and as its novelty, Al/Gr composites have been manufactured via a new novel technique, powder metallurgy and press bonding process. Then, as a function of Gr as additive part in this study, tribological, mechanical and microstructure properties of Al/Graphite composites were studied. The tribo surface and microstructure of composites have been investigated more over using SEM microscopy. The density and wear rate of samples increased and the hardness and friction coefficient decrease and by increasing the Gr content. Results showed that addition of Gr into Al matrix can improve the tribological properties of composite.

Keywords: Accumulative press bonding, Wear, Hybrid, Nano composite, Graphite

Biographical notes: **M. Heydari Vini** is currently Assistant Professor at the Department of Mechanical Engineering, Mobarakeh University, Isfahan, Iran. His current research interest includes metal forming and metal matrix composites.

Research paper

COPYRIGHTS

© 2023 by the authors. Licensee Islamic Azad University Isfahan Branch. This article is an open access article distributed under the terms and conditions of the Creative Commons Attribution 4.0 International (CC BY 4.0)

(<https://creativecommons.org/licenses/by/4.0/>)



1 INTRODUCTION

Usually Al based composites are manufactured via adding additive materials into the Al matrix contains prominent property. Graphite is one of these reinforcements [4-7]. Al based composites exhibit inadequate tribological properties under deficit lubricating conditions despite the aforementioned benefits. The trouble in adding lubrication for surfaces to enhance the wear resistance, has been the topic of many researches to produce self-lubricating material. During the wear test, Gr layer on the composite surfaces can reduce the friction and shear stresses among the composite layers [8]. To manufacture ALMCs, such as accumulative roll bonding (ARB), Many forming processes through SPD techniques are used such as cyclic extrusion compression (CEC), squeeze casting and spray forming [10].

Since cast MMCs usually have poor fracture toughness and ductility while have a desirable particle distribution through the metallic matrix. So, these problems inspire the helping of a manufacturing technique such as ARB after the stir casting process, in this study. ARB is defined as cumulative rolling processes on multi layered strips with the same primary dimensions which have been prepared which is defined by Saito in 1998 [6].

Accumulative pressing as a bonding process is defined as cumulative pressing processes. The reduction in thickness for every APB stage is 50%. The goal of this study is to fabricate Al/Gr composites to produce a uniform Gr scattering through the AA1100 matrix. The production of Al/Gr composites and focus on the trapping graphite layer through the Al matrix as a more stable self-lubricating phase during the wear process is the goal of this study at 310°C as its novelty. It was tried to fabricate Al/Gr composite and estimate the bonding, friction coefficient, density, wear resistance, microstructural and hardness.

2 EXPERIMENTAL PROCEDURE

2.1. Materials and Experimental Procedures

To fabricate aluminum-based composite in this study, Gr particles with average size 50 nm with 0, 2.5, 5 and 10 Vol.% were milled with atomized aluminum alloy 1100 with average size 30 μm in nitrogen gas as carrier. The milling process was done via a ball mill with made of stainless St vial with 10 mm diameter for 24 hours. During this process, the ball to powder weight ratio and rotational speed were 1:16 and 400 rpm, respectively. Also, 1.5 Vol.% of Stearic acid as the process control agent (PCA) was used. The resultant powder mixtures were cold pressed at a constant pressure of 750 MPa in

a steel die with dimensions of 15 and 25mm in height and diameter, respectively. Then, using a 45-ton hydraulic press at linear speed of 36 mm/min with the extrusion ratio of 11:1 and resulted in 8mm diameter extruded bars, these compacts were extruded at 550 °C for 50 minutes. Now, the final hot extruded produced Al/Graphite composite samples are ready for the next APB process.

The ASTM G99-95 standard was used for conducting the dry sliding pin on disk wear tests according samples to the investigation of the tribological behaviors of the fabricated. Before the tests, the disks and pins were polished. Using an electronic balance with a precision of 70.1 mg, the surfaces of samples were cleaned with alcohol. Then, utilizing short and long sliding distances of 400 and 1000 mm, the wear weight loss was measured, respectively [11-13]. Moreover, scanning electron microscope (SEM) was used to explore the worn surfaces of the samples.

2.2. APB process

Samples with 100 mm length, 50 mm width and 2 mm height were machined afterward making as hot extruded composites. Then, the samples were fully annealed at 450°C for 120 minutes before the APB process. Also, the samples were degreased in acetone bath for 15 minutes. In direction to eliminate the surface oxide layer, the surfaces of samples were fully brushed to guarantee an acceptable bonding between the layers. Adsorbed ions, greases, oxides and dust subdivisions are surrounded the surfaces of samples. Using a 95 mm diameter stainless steel with 0.26 mm wire diameter and speed of 2000 rpm, the sample bars were crashed after degreasing in the acetone bath. So, surface cleaning before each cumulative pressing is essential to generate a successful bonding. Then, two bars were piled together to achieve 10 mm thickness and press bonded with 50% reduction at 310°C to acquire 5mm thickness.

To handle the pressing process, a 100 tons' hydraulic press machine was used. The composite produced after one step of APB was cut into two parts and preheated at 310°C for 5 minutes. In the next step, two bars of MMCs were loaded each other after surface cleaning. The fabricated sample was cut into two bars and a pressing process with a 50% of thickness reduction repeated up to eight steps. Increasing the plastic strain during the cumulative pressing leads to a better dispersion of the powder particles. The tensile test specimens were prepared according to the ASTM-E8M standard with the length and diameters of 25 and 6 mm, respectively. The tensile strain for conducting the tensile test was $1.67 \times \frac{10^{-4}}{\text{sec}}$ on a Hounsfield H50KS testing machine. Also, the standard ASTM-E384 was utilized for doing the hardness test. Moreover, to perform the wear test on the composite samples, the wear tests performed on a pin on

flat wear testing machine with a constant rotation speed of 38 rpm. The length of each round was 16 cm and normal load (F_n) of 50 N at room temperature without lubrication with the total distance of 100 m.

3 THEORETICAL APPROACH

3.1. A theoretical model for bond strength evolution

In the proposed model by Bay (1983) [14, 15] at the normal atmospheric conditions, the mechanism of joining by plastic deformation has been theoretically explained. Based on this model, the bond strength σ_B is almost equal to the normal stress p_n (i.e. pressure) applied to the surfaces participating in joining in the absence of the surface film, Fig. 1. Accordingly, the joining strength would be:

$$\sigma_B \sim p_n. \quad (1)$$

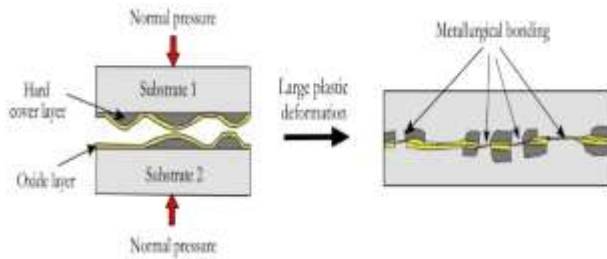


Fig. 1. drawing illustration of the bonding process based on film theory [15].

So, the effective bonding area established along the joint interface is just a fraction of the total area due to the thin oxide layer. Therefore, the obtained bond strength has to be proportional to the applied pressure through a surface expansion factor ψ to satisfy the macroscopic force equilibrium as:

$$\sigma_B = \psi p_n \quad (2)$$

Theoretically depending on the plastic deformation along the joint interface, the value of ψ may range from 0 to 1. To describe the joining by plastic deformation, Eq. 2 is the basic equation for bond strength and as the ratio between the area of the uncovered metal to the total surface area of the interface the surface expansion ψ is given by

$$\psi = \frac{A - A_0}{A} \quad (3)$$

where, A and A_0 are the areas of the joint interface for deformed and unreformed configurations, respectively. It is important to note that its impossible the bond strength be more than the yield stress of the weaker metal and expressed as:

$$\sigma_B \leq \min(\sigma_{Y1}, \sigma_{Y2}) \quad (4)$$

when, σ_{Y1} and σ_{Y2} are the yield stresses of two joining metals. Therefore, another maximum limit has to be taken as:

$$\sigma_B \leq \frac{2}{\sqrt{3}} \min(\sigma_{Y1}, \sigma_{Y2}) \quad (5)$$

3.2. Roll bonding process

Roll bonding (RB) as one of the technologies to bond the metallic laminates and composites is ran by large plastic deformation. usually, two or more layers are rolled together to produce a laminate metallic composite either at room temperature or elevated temperature, Fig. 2. Always roll bonding can provide the possibility to combine similar or dissimilar metals in many engineering applications due to the difference in their melting temperature. Because of this, many metal combinations in industry are not practically possible by fusion welding. For example, aluminum aircraft panels are manufactured using roll bonding technology and thermostat materials, many electronic contacts.

The most important factor in roll bonding processes affecting the bond strength are (1) surface cleanness (2) thickness reduction after rolling process, (3) surface cleanness, (3) rolling speed (4) pre-annealing, (5) post-annealing, etc.

For this reason, a number of investigations have been carried out during the last years to identify the parameters which may affect the bond strength of roll bonded materials. On this basis, the most important parameters affecting the bond strength are (1) thickness reduction after rolling process, (2) surface cleanness, (3) pre-annealing, (4) post-annealing, (5) rolling speed, etc. In this paper, the focus lies on the first two factors because of their importance in bond formation processes [15].

3.3. Modeling of bonding evolution

Using a cohesive zone to model non-linear fracture in different engineering applications cohesive zone modeling of separation along the interface has been conducted during the recent decades as a useful tool for describing. These applications include modeling of crystal-coating interface degradation, modeling of crack growth in composite materials, modeling of cracking in rock joints modeling of fiber reinforced concrete and modeling of delamination processes with fiber bridging. So, in the cohesive zone model describes a relation between the gap vector $g = (g_n, g_s)$ within the interface and the traction vector $t = (t_n, t_s)$, [15]. g_s and g_n are tangential and normal components of the gap vector along the interface, respectively.

As illustrated in Fig. 3a. the relative displacement between the two bodies Ω_1 and Ω_2 , the gap vector $g = (g_n, g_s)$ can be defined, Fig. 2a. Moreover, t_s and t_n

indicate the tangential and normal components of the traction vector. To describe the traction-separation relation numerous definitions have been suggested in literature depending on the modeling requirements. Based on them, polynomial and exponential, tri-linear and bi-linear models are especially worth to be mentioned, [15]. To describe the debonding process in roll bonded metal sheets a bi-linear cohesive zone model shown in Fig. 3b has been applied, in this study. According to this model, the traction between metallic layers increases linearly by more interfacial separations. So, the traction starts to reduce because of the growth of damage along the interface when the threshold value is less than the separation across the joining interface.

$$t_n = (1 - d)k_0 \langle g_n \rangle \tag{7}$$

$$t_s = (1 - d)k_0 g_s \beta^2 \tag{8}$$

Here, d and k_0 are the damage variable and interface stiffness, respectively. The constant β is a controls the contribution of the shear components in velocity tractions, Fig. 2a.

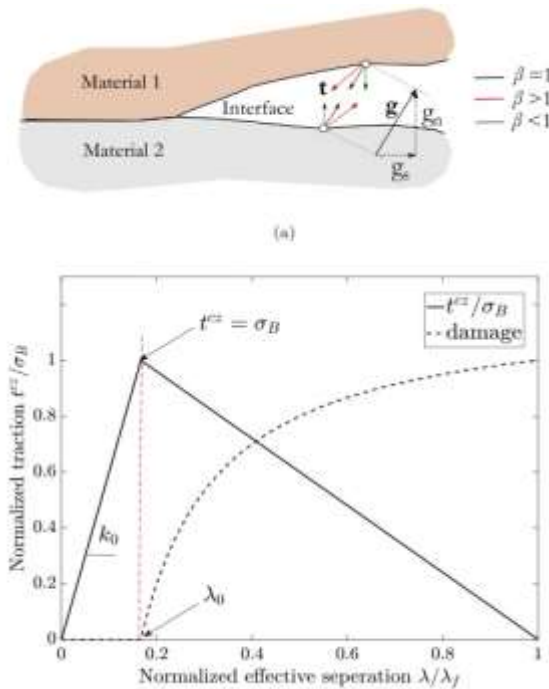


Fig. 2 (a) An interface between two materials with a gap vector g and traction vector t between two point, and (b) bi-linear traction-separation law and the evolution of damage with respect to effective separation λ , [15].

The damage evolution belongs to related to the effective separation λ as, [15]:

$$\begin{cases} 0, & \lambda < \lambda_0 \\ \frac{\lambda_f}{\lambda_f - \lambda_0} \times \frac{\lambda - \lambda_0}{\lambda} & \lambda_f < \lambda < \lambda_0 \\ 1, & \lambda_f < \lambda \end{cases} \tag{9}$$

The scalar value λ_0 indicates the threshold for the damage initiation, λ is the effective separation and λ_f is the value of effective separation at which the complete decohesion takes place scalar value λ is the effective separation, λ_0 indicates the threshold for the damage initiation and λ_f is the value of effective separation at which the complete decohesion takes place. The relation between the the effective separation λ and effective traction t^{cz} is shown in Fig. 2b. according to Fig. 2b, based on the bond strength σ_B , the effective traction has been normalized can be gain before the initiation of damage. In the present study and as an input parameter of the model, the bond strength is not considered. And the present model is able to describe both of debonding and bonding processes, Fig. 3, [15].

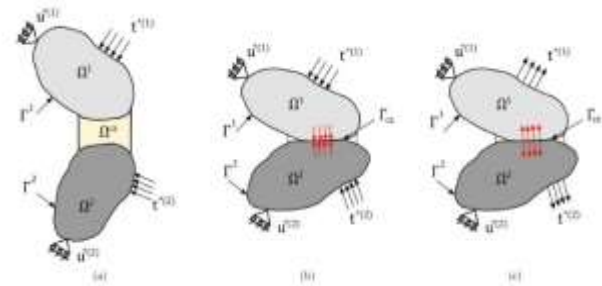


Fig. 3 Three possible situations for modeling of bonding elements, (a) before contact (b) under rolling and (c) after rolling process (separation) [15].

4 GENERAL GRAMMAR AND PREFERRED USAGE

4.1. Bonding strength

The effect of TiC Particles Wt.% on the average peeling force of composite after four ARB cycles are shown in Fig. 4. According to Fig. 4, the bond strength decreases significantly by increasing the TiC Wt. %. These particles are the main barrier in front of the pressing of virgin metals during the ARB. By increasing the TiC Particles Wt.%, the extrusion area (bonding area) of the virgin metals decreases which weaken the bonding strength.

4.2. Friction Coefficient

Gr particles may contribute in decreasing the friction coefficient during dry sliding through the tribolayer formed. Fig. 5 shows that by increasing the Gr content, the friction coefficient decreases. Gr usually acts as a

lubricant and in Al/Gr samples and the friction coefficient has a major drop due to the presence of Gr among the contacting surfaces. By increasing the Gr content more than 2.5 %, the film thickness of Gr on the composite surface increases and caused deeper penetration of the asperities which leads to generating of large resistance to movement. So, by increasing the Gr content, the wear resistance of the composite samples increases together with increasing the friction coefficient.

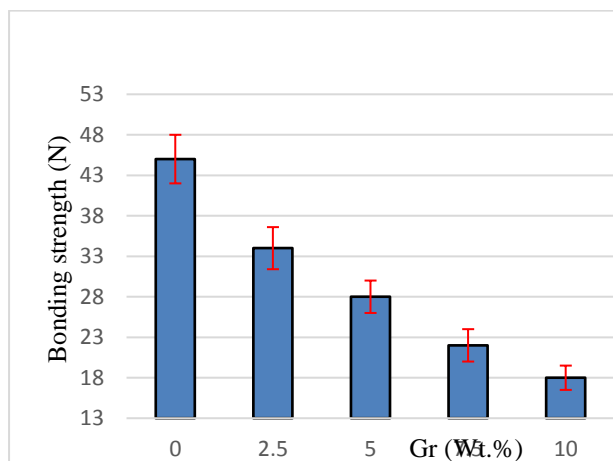


Fig. 4 The effect of TiC Particles Wt. % on the bonding strength of composite samples.

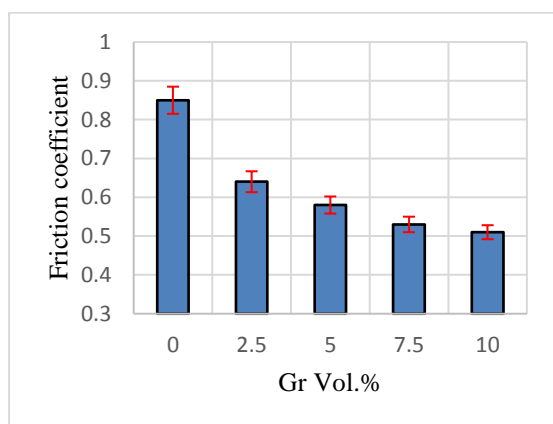


Fig. 5 The effect of Gr content on the sliding friction coefficient

Fig. 6 shows the effect of wear pin sliding velocity on the wear rates at various sliding velocities for unreinforced AA1100 and Al/Gr (7.5 Vol.% Gr) samples. According to Fig. 6, the temperature between pin and composite surface increases by increasing the sliding velocity, which accelerates the oxidation and generation of tribolayers which increases the wear rate [11].

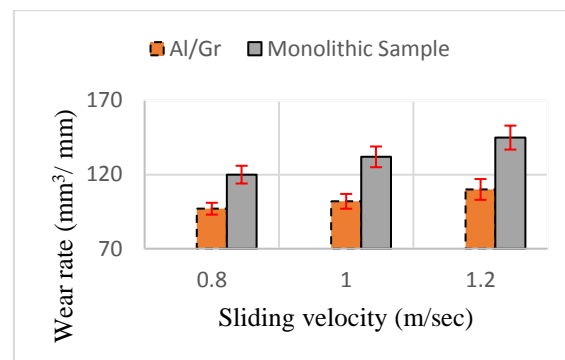


Fig. 6 The wear rate as a function of sliding velocity

This increasing in the sliding velocity leads to generation of microstructural changes inside the crystalline lattice [13]. As can be seen in Fig. 6, for all of these three composite samples, the wear rate increases by increasing the sliding velocity. The wear rate value for Al/Gr sample is higher than monolithic sample due to the effects of Gr particles.

4.3. Hardness Test

Fig. 7 shows the average Vickers micro hardness of composite samples vs various Gr contents. The average micro hardness decreases by increasing the Gr content which have been reported by other researchers, Fig. 7. Al/Gr composites with higher Gr contents exhibit lower hardness value which is due to the presence of soft graphite particles through the Al matrix that subsidize in lowering hardness values.

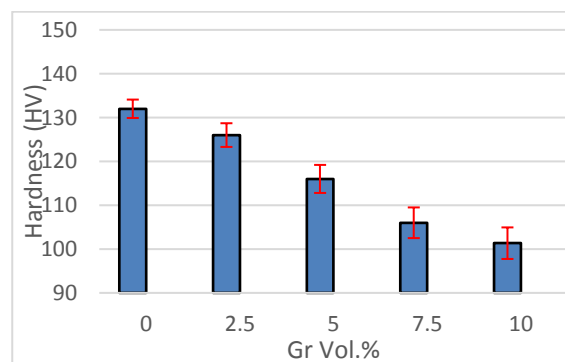


Fig. 7 The effect of Gr content on the hardness of Al/Gr composites

4.4. Density

As a function of graphite content, the relative density of the Al-based composites is shown in Fig. 8. The addition of Gr in composite material led to a significant decrease in relative density due to the considerable increasing of porosities in the samples with higher Gr content, Fig. 8, [14]. However, by increasing the graphite content up to 7 Vol.%, the relative density of both Al/Gr composites increased from 97.2 to 99.5. So, Gr can effectively reduce the inter layer friction as a solid lubricant and improves the powder flow [8, 11].

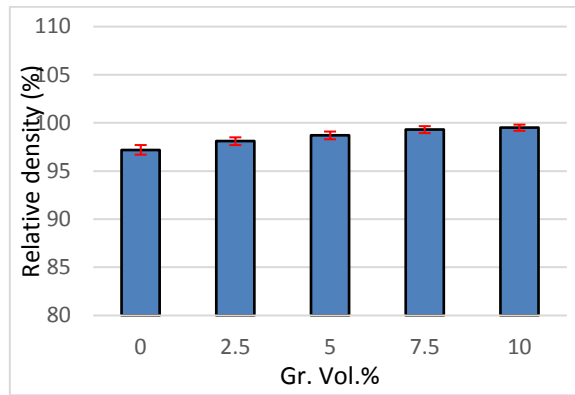


Fig. 8 The effect of Gr content on the relative density of composite samples

4.5. Wear Test

Fig. 9 shows the wear rate of samples vs Gr contents. As can be seen in Fig. 9, the wear rate of samples increases by growing the Gr content. The wear resistance of materials is a function of the hardness value based on the Archard equation and in agreement with a number of reports [10]. Increasing the Gr content as a solid lubricant in the second stage from 2.5 up to 10 Gr Vol.%, reduces the frictional forces and as a result, the wear rate decreases by reducing the metal to metal contact [7]. By increasing the Gr Vol.% the lubricating film thickness on the contact surfaces increases the mechanical properties and hardness of composites meaning the Gr can generate suitable places in bulk materials for fracture happening.

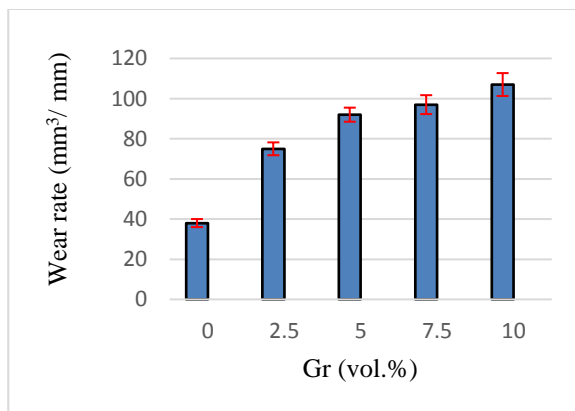


Fig. 9 The weight loss in sliding wear as a function of Gr content

4.6. Worn Surface Morphology

Fig. 10 indicates the surface morphology of composite samples fabricated after 8 steps of APB containing 2.5 and 10 Vol.% of Gr particles after the wear testing. According to Fig. 10, the wear rate of samples increases by increasing the Gr content. Also, small wear tracks are the result of abrasive wear mechanism. So during the

sliding wear test, more graphite is released to the wear surface as the amount of graphite content [11, 14]. As a result, more wear debris would be generated in composites containing higher Gr contents by reducing the friction coefficient. A black film of the lubricating layer covers the surface morphology of hybrid Nano composites and is generated as a result of shearing of Gr below the contact surfaces which changes the worn surfaces by preventing from direct contact between the pin and the counter face, Fig. 10.

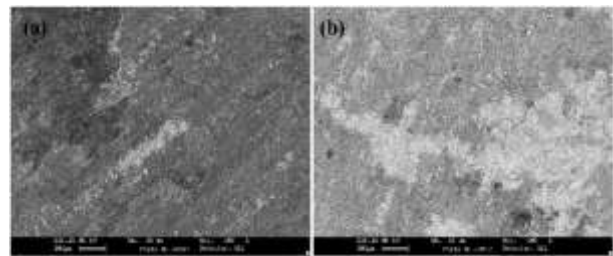


Fig. 10. SEM microphotographs of worn surface of Al/Gr samples with (a) 2.5 and (b) 10 Vol.% of Gr particles

5 CONCLUSION

The investigation of the tribological behavior of Nano hybrid Al/Gr composites was the main purpose of this study. Wear test, hardness test and SEM analysis were performed and the following results were attained:

1. Due to the soft phase (Gr particles) embedded uniformly in the Al based matrix, Al/Gr composites as showed lower hardness compared to monolithic samples.
2. The wear rate of monolithic samples was more than Al/Gr within the observed range of sliding velocities.
3. The wear rate of composites increases with increasing the Gr particles.
4. With higher Gr Vol.% contents, the hardness value decreases due to the slippery and soft nature of Gr.

REFERENCES

[1] Heydari Vini, M., A new rolling pressure model for an actual reversing cold rolling strip mill, ADMT Journal, Vol. 8, No. 2, 2015 pp. 73-80

[2] Heydari Vini, Sedighi, M., Mondali, M., Mechanical Properties, Bond Strength And Microstructural Evolution Of AA1060/TiO₂ Composites Fabricated By Warm Accumulative Roll Bonding (WARB), Journal of Materials Research, Vol. 108, No. 1, 2017, pp. 53-59.

[3] Amir Khanlou, S., Jamaati, R., Niroumand, B., Toroghinejad, M. R., Using ARB Process as A Solution for Dilemma of Si and SiC P Distribution in Cast Al – Si

- / Sic P Composites, Journal of Materials Processing Technology, Vol. 211, 2011, pp. 1159–1165.
- [4] Jamaati, R., Toroghinejad, M. R., Manufacturing of High-Strength Aluminum / Alumina Composite by Accumulative Roll Bonding. Materials Science & Engineering A, Vol. 527, No. 16-17, 2010, pp. 4146–4151.
- [5] Vini, MH., Daneshmand, S., Effect of Electrically Assisted Accumulative Roll Bonding (EARB) Process on the Mechanical Properties and Microstructure Evolution of AA5083/Al₂O₃ Composites, Materials Performance and Characterization, Vol. 8, No. 1, 2019, PP.594-603
- [6] Alizadeh, M., Talebian, M., Fabrication Of Al/Cup Composite By Accumulative Roll Bonding Process And Investigation Of Mechanical Properties, Materials Science and Engineering A, Vol. 558, 2012, pp. 331–337.
- [7] Heydari Vini, M., Sedighi, M., Mondali, M., Mechanical properties and microstructural evolution of AA5083/Al₂O₃ composites fabricated by warm accumulative roll bonding, ADMT Journal Vol. 9, No. 4, 2016, pp.13-22.
- [8] Korbel, A., Richert, M., Richert, J., The Effects Of Very High Cumulative Deformation On Structure And Mechanical Properties Of Aluminium, in: Proc. Second RISO Int. Symp. Metall. Mater. Sci., 1981, pp. 14–18.
- [9] Farhadipour, P., Sedighi, M., Heydari, M., Using Warm Accumulative Roll Bonding Method to Produce Al-Al₂O₃, Proceedings of the Institution of Mechanical Engineers Part B Journal of Engineering Manufacture Vol. 231, No. 5, 2017, pp. 889-896.
- [10] Ipek, R., Adhesive Wear Behaviour of B₄C and Sic Reinforced 4147 Al Matrix Composites (Al/B₄C-Al/SiC), J. Mater. Process. Technol, Vol. 162-163, 2005, pp.71-75.
- [11] Vini, MH., Daneshmand, S., EFFECT OF TiO₂ PARTICLES ON THE MECHANICAL AND MICROSTRUCTURAL EVOLUTION OF HYBRID ALUMINUM-BASED COMPOSITES FABRICATED BY ..., Surface Review and Letters, Vol. 27, No. 12, 2020, PP. 2050026
- [12] Alizadeh, M., Comparison of Nanostructured Al / B₄C Composite Produced by ARB and Al / B₄C Composite Produced by RRB Process, Materials Science & Engineering A, Vol. 528, No. 2, 2010, PP. 578–582.
- [13] Vini, MH., Daneshmand, S., Effect of TiO₂ particles on the mechanical, bonding properties and microstructural evolution of AA1060/TiO₂ composites fabricated by WARB, Advances in materials Research, Vol. 9, No. 2, 2020, PP. 99-107
- [14] Sedighi, M., Vini, M. H., Farhadipour, P., Effect of Alumina Content On the Mechanical Properties of AA5083/Al₂O₃ Composites Fabricated by Warm Accumulative Roll Bondingm, Powder Metallurgy and Metal Ceramics, Vol. 55, No. 510, 2016, PP. 413–418.
- [15] Khaledi, K., Rezaei, S., Wulfinghoff, S., & Reese, S., Modeling of joining by plastic deformation using a bonding interface finite element. International Journal of Solids and Structures, Vol. 160(October), 2019, PP. 68–79.